Penerbit Akademia Baru

Journal of Advanced Research in Micro and Nano Engineering

Journal homepage:
https://www.akademiabaru.com/submit/index.php/armne/index
ISSN: 2756-8210

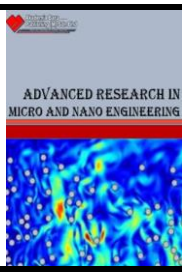

Unary Adsorption Isotherm of Carbon Dioxide and Methane of Nickel Gallate Metal-organic Framework

Marhaina Ismail[1], Mohamad Azmi Bustam[2,*], Yeong Yin Fong[1], Aqeel Ahmad[3]

[1] Carbon Dioxide Research Centre (CO_2RES), Universiti Teknologi PETRONAS, 32610 Bandar Seri Iskandar, Perak, Malaysia
[2] Centre of Research in Ionic Liquids (CORIL), Universiti Teknologi PETRONAS, 32610 Bandar Seri Iskandar, Perak, Malaysia
[3] Interdisciplinary Research Center for Refining and Advanced Chemicals, King Fahd University of Petroleum and Minerals, Dhahran 31261, Saudi Arabia

ARTICLE INFO

Article history:
Received 23 January 2024
Received in revised form 15 March 2024
Accepted 27 April 2024
Available online 30 May 2024

Keywords:
Adsorption; MOF; isotherm; thermodynamic; kinetic

ABSTRACT

Carbon dioxide (CO_2) and methane (CH_4) adsorption using metal-organic frameworks (MOFs) has garnered continuous interest in academia and industrial fields due to their remarkable performances. A series of studies have been dedicated to design the potential MOFs for CO_2 and CH_4 adsorption. Among them, nickel gallate MOF (Ni-gallate) can act as a promising adsorbent based on the predicted adsorption capacity and selectivity. However, the behaviors of CO_2 and CH_4 unary adsorption isotherms of Ni-gallate have not been studied by isotherm and kinetic models. Therefore, the aim of this work is to perform pure CO_2 and CH_4 gas adsorption and the unary adsorption isotherms were explained by the isotherm and kinetic models. Based on the unary adsorption isotherms, CO_2 adsorption capacity values were observed to be higher than CH_4 which resulted in great selectivity values. For isotherm models, the Toth model demonstrated the highest goodness-of-fit compared to Langmuir, Freundlich and Sips models and the thermodynamic properties were determined using its constant values. On the other hand, the kinetic data was best-fitted by the pseudo-first order model compared to the pseudo-second order and Elovich models and its constant values were used to determine activation energy. This useful information is very important for the design and operation of CO_2 and CH_4 adsorption systems.

1. Introduction

Adsorption is a surface phenomenon that occurs when the adsorbate attaches physically (physisorption) or chemically (chemisorption) to the surface of an adsorbent. Physisorption (physical adsorption) is based on the attraction forces between the solid phase and gas phase with a relatively low adsorption heat. The physical adsorption is caused by a weak bond like Van der Waals force or electrostatic force. Chemisorption (chemical adsorption) occurs due to the formation of strong chemical bonds. Owing to the weak forces involved in physisorption, adsorption can be easily reversed. This is also called desorption which is the removal of the adsorbed molecules from the

* *Corresponding author.*
E-mail address: azmibustam@utp.edu.my

https://doi.org/10.37934/armne.19.1.5162

surface of the adsorbent. Adsorption is highly dependent on the solid adsorbents such as zeolite and activated carbon. Nowadays, metal-organic frameworks (MOFs) have emerged as promising adsorbents for various applications such as gas separation, storage and catalysis since they have the advantages of large surface area, great porosity, tailorable pore size, tunable geometry and structure, and stability [1,2].

Adsorption presents the opportunity for energy savings with reduced capital and operational expenses when contrasted with alternative technologies like absorption, membrane, and cryogenic. In addition, absorption is known to face the drawbacks such as equipment corrosion and high energy consumption [3]. The membrane is difficult to maintain the material performance since it has poor durability [4]. Cryogenic is a complex process, high cost and requires high energy consumption [5]. Adsorption also stands out as the preferred process due to its simplicity in operation [6,7].

The unary adsorption isotherm stands out as a fundamental concept in the field of adsorption. Unary adsorption isotherm is very essential to understand the equilibrium performance of solid adsorbent in describing how much the adsorbate can attach onto the surface of adsorbent. It elucidates the interaction behaviors between the adsorbent and adsorbate at a fixed temperature, expressing the relationship as the amount of adsorbate in relation to partial pressure. Therefore, it has the capability to ascertain the adsorption capacity of the adsorbent for a certain adsorbate under equilibrium conditions. The unary adsorption isotherm serves as a fundamental step in characterizing the adsorption behavior and provides essential data for the design and optimization of adsorption process. Consequently, isotherm models and kinetic models can appropriately fit the experimental unary adsorption isotherm, predicting adsorption behaviors. This understanding and interpretation of adsorption isotherms are crucial, as these models provide mechanism and reaction rate information essential for designing various adsorption processes [8].

According to our previous reported work, Grand Canonical Monte Carlo (GCMC) simulation suggested that the nickel gallate metal-organic framework (Ni-gallate) has the potential to serve as a cost-effective adsorbent for the separation of CO_2 and CH_4 based on the predicted unary adsorption isotherms [9]. In addition, Ni-gallate demonstrated remarkable performance in CO_2 and CH_4 adsorption, as indicated by experimental unary adsorption isotherms [10]. However, its adsorption behaviors are not adequately explained by any isotherm and kinetic models. Therefore, the primary aim of this study is to synthesize Ni-gallate and conduct adsorption experiments with pure CO_2 and CH_4 gases. The CO_2 and CH_4 adsorption behaviors of Ni-gallate were described by using various equilibrium adsorption isotherm models including Langmuir, Freundlich, Sips, and Toth models. The thermodynamic properties were determined based on the best-fitted isotherm model constants. On the other hand, the kinetic information was derived by fitting the experimental data to the pseudo-first order, pseudo-second order, and Elovich models. The activation energy was computed using the constants obtained from the best-fitted kinetic model. The equilibrium adsorption behaviors described by these models are expected to provide mechanism and reaction rate information, guiding the future design and operation of CO_2/CH_4 adsorption processes using Ni-gallate.

2. Methodology

2.1 Hydrothermal Synthesis of Ni-gallate

The hydrothermal synthesis of Ni-gallate was conducted following the procedure outlined in the previous work [11]. A 250 mL of 0.16 M of potassium hydroxide solution was prepared and transferred into a 1 L round-bottomed flask. 0.05 mol of nickel (II) chloride anhydrous and 0.1 mol of gallic acid were mixed into the flask and the reaction was conducted at 353 K. After 24 hours, the mixture was cooled until two layers formed. The mother liquor (upper layer) was decanted, and the

solid product was rinsed twice with deionized water. The product was immersed in ethanol for two days, with ethanol replenished twice daily. The product underwent treatment using a pretreatment unit before undergoing characterization analysis including Fourier Transform Infrared Spectroscopy (FTIR), Powder X-ray Diffraction (PXRD) and Surface Area and Porosity (SAP). The analysis methodologies were referenced from the reported literature [12].

2.2 CO_2 and CH_4 Pure Gas Adsorption

The CO_2 and CH_4 pure gas adsorption experiments were performed using a commercial unit, the 3FLEX Micromeritics Surface Characterization, at three different temperatures (273 K, 298 K, 313 K) and pressure up to 1 bar. Prior to the adsorption measurements, the sample was subjected to degassing at 393 K for a duration of 24 hours.

2.3 Isotherm Models

The experimental unary adsorption isotherms for CO_2 and CH_4 were fitted using four different isotherm models, as tabulated in Table 1.

Table 1
Isotherm models

Model	General Form	Linear Form	Reference
Langmuir	$q_e = \frac{q_m K_L P_e}{1 + K_L P_e}$	$\frac{P_e}{q_e} = \frac{P_e}{q_m} + \frac{1}{K_L q_m}$	[13,14]
Freundlich	$q_e = K_F P_e^{1/n}$	$\log q_e = \log K_F + \frac{1}{n} \log P_e$	[14,15]
Sips	$q_e = \frac{q_m (K_S P_e)^{1/n}}{1 + (K_S P_e)^{1/n}}$	$\ln\left(\frac{q_e}{q_m - q_e}\right) = \frac{1}{n} \ln P_e + \ln (K_S^{1/n})$	[16,17]
Toth	$q_e = \frac{q_m K_T P_e}{[1 + (K_T P_e)^n]^{1/n}}$	$\ln \left(\frac{q_e^n}{q_m^n - q_e^n}\right) = n \ln P_e \ + n \ln K_T$	[18,19]

where P_e is the equilibrium pressure, q_e is the adsorption capacity at equilibrium, q_m is the maximum adsorption capacity and n is the heterogeneity factor. K_L, K_F, K_S and K_T denote the constants associated with respective models.

The thermodynamic properties can be obtained using van Hoff's formulation as shown below [20]

$$\Delta G° = \Delta H° - T.\Delta S° \quad (1)$$

$$\Delta G° = -RT \ln k_{eq} \quad (2)$$

where k_{eq} is the isotherm model constant, *T* is the temperature and the universal gas constant is signified by *R*. $\Delta G°$ is the change in Gibbs free energy, $\Delta H°$ is the change in enthalpy of reaction and $\Delta S°$ is the change in entropy of adsorbent-adsorbate interaction.

2.4 Kinetic Models

In order to perform kinetic studies on CO_2 and CH_4 adsorption, the following three common models were employed as summarized in Table 2.

Table 2
Kinetic models

Model	General Form	Linear Form	Reference
Pseudo-first order	$q_t = q_e(1 - e^{-k_f t})$	$\log(q_e - q_t) = \log(q_e) - (\frac{k_f}{2.303})t$	[21,22]
Pseudo-second order	$q_t = \frac{q_e^2 k_s t}{1 + q_e k_s t}$	$\frac{t}{q_t} = \frac{t}{q_e} + \frac{1}{k_s q_e^2}$	[21,22]
Elovich	$q_t = \frac{1}{\beta}\ln(1 + \alpha\beta t)$	$q_t = \frac{1}{\beta}\ln(\alpha\beta) + \frac{1}{\beta}\ln t$	[23,24]

where q_e is the adsorption capacity at equilibrium, q_t is the adsorption capacity at t (time). k_f, k_s and α are the rate constants for respective models, while β is the desorption constant.

The activation energy (E_a) can be determined based on the rate constant using Arrhenius equation as follows [25]

$$k = Ae^{-(\frac{E_a}{RT})} \tag{3}$$

where k is the rate constant and A is the pre-exponential factor.

3. Results

3.1 Characterization Analysis

The results of Fourier Transform Infrared Spectroscopy (FTIR), Powder X-ray Diffraction (PXRD), and Surface Area and Porosity (SAP) analyses are presented below.

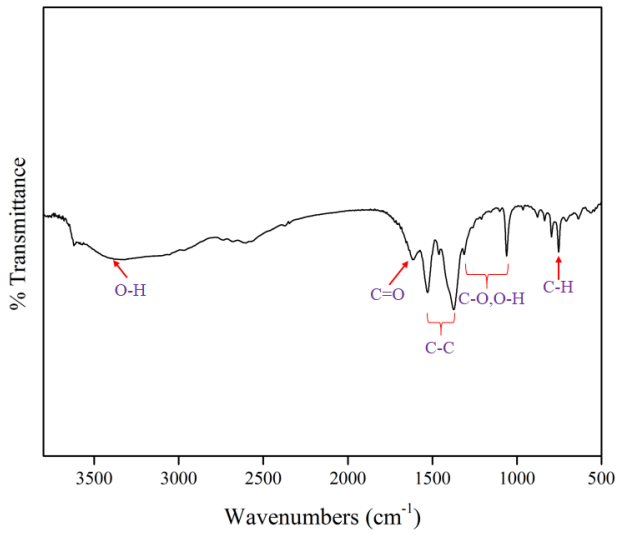

Fig. 1. FTIR spectrum of Ni-gallate

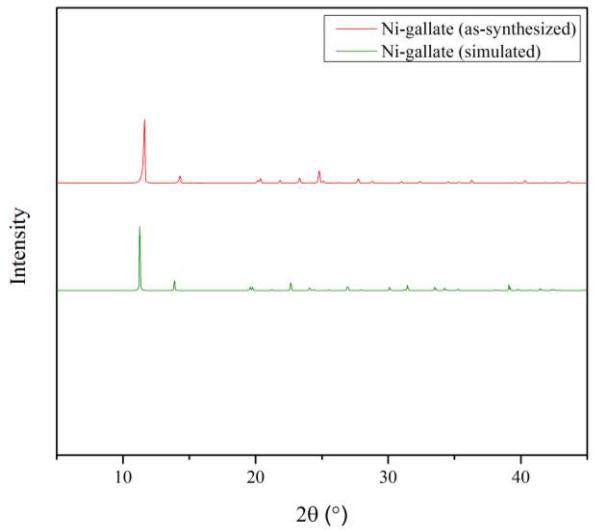

Fig. 2. PXRD pattern of Ni-gallate

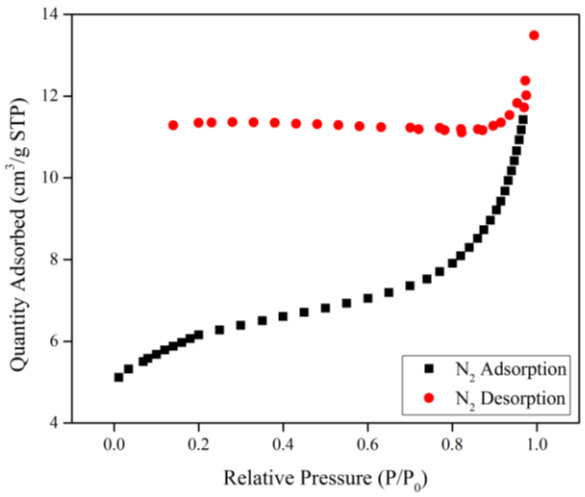

Fig. 3. N_2 adsorption-desorption of Ni-gallate

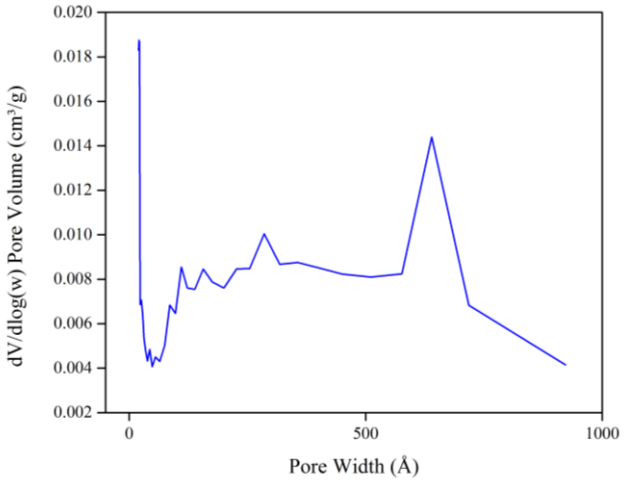

Fig. 4. BJH pore size distribution of Ni-gallate

The FTIR spectrum in Figure 1 reveals peaks corresponding to functional groups of Ni-gallate. The peaks located at 3500-2800 cm^{-1} indicated the presence of O-H of carboxyl group. At 1616 cm^{-1}, C=O of carboxyl group has appeared. C-C bonds in aromatic structure of gallic acid were confirmed at 1530, 1462 and 1376 cm^{-1}. Peaks in the range of 1300-1000 cm^{-1} presented C-O and O-H bonds of the aromatic rings. The peak for C-H bond of the aromatic ring was found to be at 750 cm^{-1}. These findings align well with the results reported in the earlier study [12].

The PXRD pattern in Figure 2 illustrates peaks corresponding to Ni-gallate at 11.53°, 14.29°, 20.23°, 21.91°, 23.33°, 24.74°, 26.25°, 27.76°, 28.84°, 31.02°, 32.36°, 34.54°, 35.38°, 36.37°, 39.63°, with additional peaks observed after 40°. These peaks align well with the literature [26]. The calculated average crystalline size of Ni-gallate is 58.2 nm. This parameter is determined by using Debye-Scherrer equation [27]. The Ni-gallate pattern was constructed using the reference structure found in the Cambridge Crystallographic Data Centre (CCDC). Its database identifier is GELVEZ and the deposition number is 286498. It shows differences in peak intensity compared to the as-synthesized pattern. This difference may be attributed to non-uniform distribution of elements in the crystal structure of the as-synthesized Ni-gallate. In general, the intensity of diffraction peaks correlates directly with the amount of elements present in the material [28].

Figure 3 illustrates nitrogen (N_2) sorption isotherms, while Figure 4 depicts the Barrett-Joyner-Halenda (BJH) pore size distribution, used to assess the surface properties of Ni-gallate. N_2 sorption isotherm was measured to determine the Brunauer-Emmett-Teller (BET) surface area, which was calculated within the relative pressure range of 0.00-0.25, yielding a value of 20.36 m^2/g. The pore volume of Ni-gallate was determined to be 0.005 m^3/g. Additionally, the BJH model estimated the pore size to be 8.52 nm.

3.2 Experimental Unary Adsorption Isotherm

Figure 5 illustrates the experimental unary adsorption isotherms of CO_2 and CH_4 of Ni-gallate at temperatures of 273, 298, and 313 K.

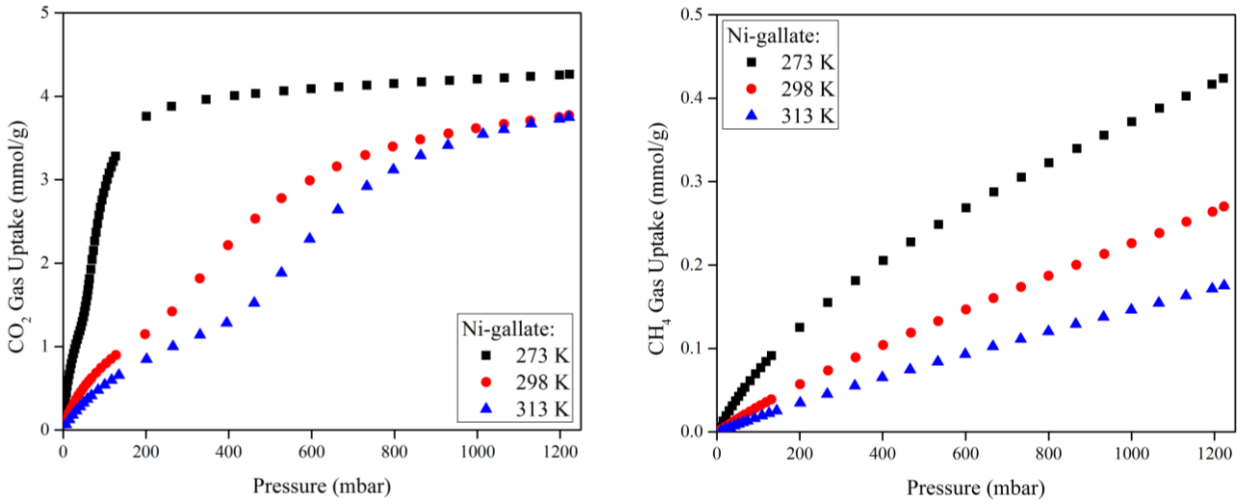

(a) (b)

Fig. 5. Experimental unary adsorption isotherms at 273, 298 and 313 K for (a) CO_2 and (b) CH_4

CO_2 uptake increased with pressure until reaching a plateau equilibrium. At an early stage of adsorption, CO_2 molecules rapidly attached to the surface of Ni-gallate, utilizing available vacant active sites. Subsequently, the active sites gradually became occupied until saturation was achieved, indicating no further adsorption occurred. On the other hand, CH_4 isotherm continued to increase with pressure without reaching saturation, illustrating that Ni-gallate can sustain higher CH_4 uptake at higher pressure conditions.

The CO_2 and CH_4 uptakes decreased with temperature, with the highest values observed at 273 K. This decrease is attributed to the weakening of adsorbent-adsorbate interactions, leading to more repulsion and a shift in equilibrium toward desorption at higher temperatures [20]. Furthermore, the higher temperature initiated the gas molecules to exhibit unsteady movement, complicating their ability to attach to the surface of Ni-gallate. The adsorbed amount of CO_2 and CH_4 declined with increasing temperature, reflecting the exothermic nature of the adsorption process. Table 3 tabulates the adsorption capacity values at three different temperatures and 1 bar.

Table 3
Adsorption capacity and selectivity of Co-gallate at 1 bar

Temperature (K)	Adsorption Capacity (mmol/g)		Selectivity
	CO_2	CH_4	
273	4.21	0.372	11.32
298	3.62	0.226	16.02
313	3.55	0.146	24.32

These adsorption capacity values play a key role in determining selectivity, providing crucial information about the potential performance of Ni-gallate in the separation of CO_2/CH_4 binary mixtures. As depicted in Table 3, Ni-gallate demonstrates promising selectivity, which is essential for real-world applications in CO_2/CH_4 separation.

3.3 Isotherm Models

The adsorption mechanism can be predicted using isotherm models that describe the interaction between Ni-gallate and gas molecules. The experimental CO_2 and CH_4 unary adsorption isotherms were fitted using two-parameter models namely, Langmuir and Freundlich as well as three-

parameter models, which are Sips and Toth models. Table 4 summarizes the model parameter values for each model studied in this work.

Table 4
Isotherm model parameters

Model	Parameter	CO_2			CH_4		
		273 K	298 K	313 K	273 K	298 K	313 K
Langmuir	K_L	0.01148	1.52×10^{-3}	3.5×10^{-4}	9.0×10^{-4}	3.3×10^{-4}	1.8×10^{-4}
	q_m	4.7393	6.0056	13.3455	0.7892	0.9138	0.9617
	R^2	0.9679	0.9938	0.9874	0.9980	0.9990	0.9998
Freundlich	K_F	0.19284	0.03707	0.01052	2.75×10^{-3}	5.8×10^{-4}	2.2×10^{-4}
	n	1.9940	1.4390	1.1346	1.4017	1.1562	1.0575
	$1/n$	0.5015	0.6949	0.8814	0.7134	0.8649	0.9456
	R^2	0.7669	0.9135	0.8450	0.9981	0.9998	0.9976
Sips	K_S	0.01368	3.19×10^{-3}	2.78×10^{-3}	1.7×10^{-4}	1.4×10^{-4}	1.1×10^{-4}
	q_m	4.3395	4.3114	4.0933	1.9706	1.7077	1.4712
	n	0.7205	0.7610	0.7986	1.2452	1.0493	1.0288
	$1/n$	1.3888	1.3141	1.2522	0.8031	0.9530	0.9720
	R^2	0.9840	0.9854	0.9033	0.9993	0.9996	0.9997
Toth	K_T	7.36×10^{-3}	1.49×10^{-3}	1.03×10^{-3}	2.6×10^{-4}	7.6×10^{-5}	4.5×10^{-5}
	q_m	4.1395	3.8013	3.7955	5.2667	4.9217	4.1876
	n	3.5180	4.1189	8.8125	0.3648	0.4937	0.5912
	R^2	0.9936	0.9909	0.9929	0.9998	0.9993	0.9999

The Toth model exhibited the highest goodness-of-fit, as evidenced by the highest correlation coefficient (R^2). The Toth model constant (K_T) values for CO_2 adsorption were found to be higher than CH_4, indicating a favorable interaction of CO_2 molecules with Ni-gallate and resulting in a higher adsorption capacity. However, the K_T values decreased with temperature, consistent with the exothermic nature of adsorption and the observed decrease in adsorbed amounts with temperature. In addition, the heterogeneity factor (n) values for CO_2 adsorption were observed to be greater than CH_4, leading to a stronger degree of surface heterogeneity. Greater heterogeneity is desirable since it enhances the adsorbent-adsorbate interaction, promoting more adsorption. Consequently, CO_2 and CH_4 adsorption occurred on the heterogeneous surface of Ni-gallate.

3.4 Thermodynamic Properties

The thermodynamic properties of CO_2 and CH_4 adsorption on Ni-gallate were obtained by plotting the linear plot as displayed in Figure 6.

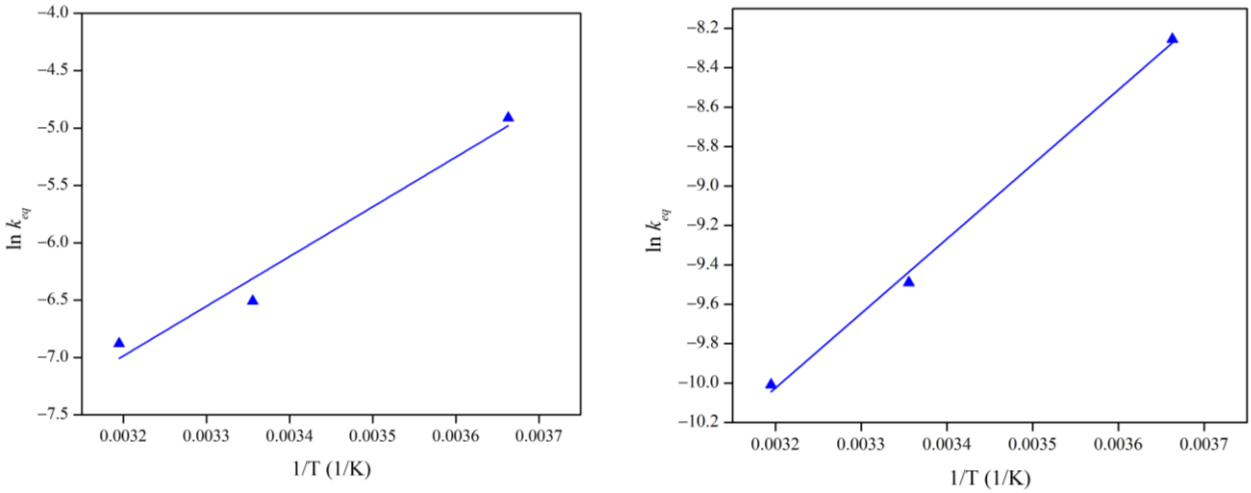

(a) (b)

Fig. 6. Van Hoff's linear plot for (a) CO_2 and (b) CH_4

Table 5 tabulates the thermodynamic properties calculated using the Van Hoff's formulation.

Table 5
Thermodynamic properties

Adsorbate	$\Delta \boldsymbol{H}°$ (kJ/mol)	$\Delta \boldsymbol{S}°$ (kJ/mol.K)	$\Delta \boldsymbol{G}°$ (kJ/mol)		
			273 K	298 K	313 K
CO_2	-36.03	-0.173	11.30	15.64	18.24
CH_4	-31.45	-0.184	18.78	23.38	26.14

The negative values of $\Delta H°$ reflected the CO_2 and CH_4 adsorption were exothermic, indicating the release of heat during the process. Besides, $\Delta H°$ serves to differentiate the nature of adsorption, distinguishing between physisorption and chemisorption. For physisorption, the magnitude of $\Delta H°$ typically falls within the range of 0-40 kJ/mol [29]. CO_2 and CH_4 adsorption were confirmed as physisorption, yielding values of -36.03 and -31.45 kJ/mol respectively. Meanwhile, the negative magnitudes of $\Delta S°$ demonstrated a reduction in randomness at the solid-gas interface during CO_2 and CH_4 adsorption on Ni-gallate. In addition, the positive values of $\Delta G°$ revealed that the adsorption process of CO_2 and CH_4 was non-spontaneous.

3.5 Kinetic Studies

The kinetic studies of CO_2 and CH_4 adsorption were investigated by correlating the adsorbed amount against time, as presented in Figure 7.

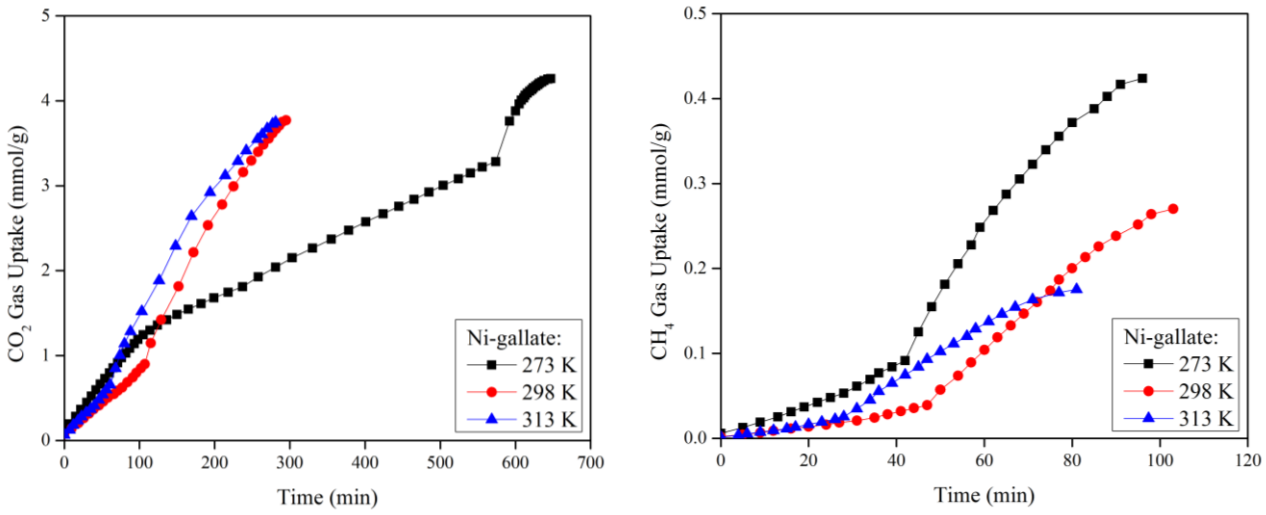

(a) (b)

Fig. 7. Gas uptake versus time at 273, 298 and 313 K for (a) CO_2 and (b) CH_4

The parameter values for the kinetic models obtained by fitting the experimental data, are presented in Table 6.

Table 6
Kinetic model parameters

Model	Parameter	CO_2			CH_4		
		273 K	298 K	313 K	273 K	298 K	313 K
Pseudo-first order	q_e	4.1677	3.7102	3.7000	0.4211	0.2690	0.1744
	k_f	2.99 x 10^{-3}	2.07 x 10^{-3}	2.76 x 10^{-3}	4.42 x 10^{-3}	2.30 x 10^{-3}	4.26 x 10^{-3}
	R^2	0.9990	0.9989	0.9918	0.9963	0.9988	0.9970
Pseudo-second order	q_e	1.6929	1.4213	1.3417	0.1474	0.0625	0.0563
	k_s	8.14 x 10^{-3}	6.51 x 10^{-3}	9.10 x 10^{-3}	0.1172	0.2246	0.3082
	R^2	0.8234	0.8731	0.7806	0.7237	0.8088	0.8811
Elovich	α	0.0582	0.0326	0.0414	6.47 x 10^{-3}	2.32 x 10^{-3}	2.59 x 10^{-3}
	β	3.3333	4.2918	4.5746	51.2821	133.3333	156.2500
	R^2	0.9065	0.9368	0.9032	0.9346	0.9499	0.9641

The pseudo-first order model demonstrated the best fit to the experimental data, as evidenced by the R^2 values exceeding 0.99. The highest adsorption rate constants for CO_2 and CH_4 were observed at 273 K, measuring 2.99 x 10^{-3} and 4.42 x 10^{-3} min^{-1} respectively, indicating the fastest adsorption kinetics among the studied temperatures. However, there was a fluctuation observed between 298 K and 313 K. Nevertheless, the adsorbed amount of CO_2 and CH_4 at 298 K remained greater than 313 K. Conversely, pseudo-second order model presented the poorest goodness-of-fit among the studied kinetic models. This model is typically more suited to explain chemisorption, suggesting that no chemisorption occurred in this case.

3.6 Activation Energy

The Arrhenius equation was employed to calculate the activation energy (E_a) of CO_2 and CH_4 adsorption, with rate constants derived from the pseudo-first-order model, given its superior goodness-of-fit. The calculated E_a for CO_2 adsorption was found to be -2.55 kJ/mol, while it was -2.91 kJ/mol for CH_4. These low E_a values suggest a low energy requirement, consistent with physisorption, which relies on weak forces like van der Waals forces [30]. Moreover, the negative

values of E_a for CO_2 and CH_4 adsorption confirmed the exothermic nature of the process, indicating enhanced adsorption at lower temperatures.

4. Conclusions

Ni-gallate demonstrated potential as an adsorbent in CO_2 and CH_4 adsorption, exhibiting a higher CO_2 adsorption capacity than CH_4 and resulting in remarkable selectivity based on the unary adsorption isotherms. The experimental unary adsorption isotherms were further subjected to fitting with isotherm and kinetic models to characterize the behaviors of CO_2 and CH_4 adsorption. Among the studied isotherm models, Toth model provided the best fit, and its constant values were applied to ascertain the thermodynamic properties. Toth model suggested that CO_2 and CH_4 adsorption occurred on the heterogeneous surface of Ni-gallate. In contrast, the kinetic data was best-fitted by the pseudo-first order model, and its constant values were employed to determine activation energy. The resulting thermodynamic properties and activation energy verified that CO_2 and CH_4 adsorption was physisorption and exothermic process. These valuable findings are expected to benefit for the future design and operation of systems involving CO_2 and CH_4 adsorption using Ni-gallate.

Acknowledgement

The funding for this research was provided through a grant from Yayasan Universiti Teknologi PETRONAS (YUTP Grant 015LC0-364). This research received support from Carbon Dioxide Research Centre (CO_2RES) and Centre of Research in Ionic Liquids (CORIL) at Universiti Teknologi PETRONAS.

References

[1] Abid, Hussein Rasool, Aamir Hanif, Alireza Keshavarz, Jin Shang, and Stefan Iglauer. "CO2, CH4, and H2 adsorption performance of the metal–organic framework HKUST-1 by modified synthesis strategies." *Energy & Fuels* 37, no. 10 (2023): 7260-7267. https://doi.org/10.1021/acs.energyfuels.2c04303

[2] Li, Chen-Ning, Shi-Ming Wang, Zhi-Peng Tao, Lin Liu, Wei-Guo Xu, Xue-Jun Gu, and Zheng-Bo Han. "Green synthesis of MOF-801 (Zr/Ce/Hf) for CO2/N2 and CO2/CH4 separation." *Inorganic Chemistry* 62, no. 20 (2023): 7853-7860. https://doi.org/10.1021/acs.inorgchem.3c00560

[3] Chen, Changwei, Xiangbo Feng, Qing Zhu, Rui Dong, Rui Yang, Yan Cheng, and Chi He. "Microwave-assisted rapid synthesis of well-shaped MOF-74 (Ni) for CO2 efficient capture." *Inorganic chemistry* 58, no. 4 (2019): 2717-2728. https://doi.org/10.1021/acs.inorgchem.8b03271

[4] Song, Chunfeng, Qingling Liu, Shuai Deng, Hailong Li, and Yutaka Kitamura. "Cryogenic-based CO2 capture technologies: State-of-the-art developments and current challenges." *Renewable and sustainable energy reviews* 101 (2019): 265-278. https://doi.org/10.1016/j.rser.2018.11.018

[5] Shen, Minghai, Lige Tong, Shaowu Yin, Chuanping Liu, Li Wang, Wujun Feng, and Yulong Ding. "Cryogenic technology progress for CO2 capture under carbon neutrality goals: A review." *Separation and Purification Technology* 299 (2022): 121734. https://doi.org/10.1016/j.seppur.2022.121734

[6] Theng, Mary Lina, Lian See Tan, and Wen Chun Siaw. "Adsorption of methylene blue and Congo red dye from water onto cassava leaf powder." *Progress in Energy and Environment* (2020): 11-21.

[7] Ahmad, Aqeel, Bryan Pango, Marhaina Ismail, and Mohamad Azmi Bustam. "Performance Evaluation of the Developed MOF-177 for CO2 Capture." *Journal of Advanced Research in Applied Mechanics* 111, no. 1 (2023): 74-81.

[8] Ismail, Marhaina, Mohamad Azmi Bustam, and Yin Fong Yeong. "Adsorption of Carbon Dioxide and Methane on Cobalt Gallate-Based Metal-Organic Framework (Co-Gallate): Equilibrium Isotherm, Thermodynamic and Kinetic Studies." *Journal of Advanced Research in Fluid Mechanics and Thermal Sciences* 108, no. 2 (2023): 151-163. https://doi.org/10.37934/arfmts.108.2.151163

[9] Ismail, Marhaina, Mohamad Azmi Bustam, and Nor Ernie Fatriyah Kari. "Screening of gallate-based metal-organic frameworks for single-component CO2 and CH4 gas." In *E3S Web of Conferences*, vol. 287, p. 02005. EDP Sciences, 2021. https://doi.org/10.1051/e3sconf/202128702005

[10] Chen, Fuqiang, Jiawei Wang, Lidong Guo, Xinlei Huang, Zhiguo Zhang, Qiwei Yang, Yiwen Yang, Qilong Ren, and Zongbi Bao. "Carbon dioxide capture in gallate-based metal-organic frameworks." *Separation and Purification Technology* 292 (2022): 121031. https://doi.org/10.1016/j.seppur.2022.121031
[11] Bao, Zongbi, Jiawei Wang, Zhiguo Zhang, Huabin Xing, Qiwei Yang, Yiwen Yang, Hui Wu et al. "Molecular sieving of ethane from ethylene through the molecular cross-section size differentiation in gallate-based metal–organic frameworks." *Angewandte Chemie* 130, no. 49 (2018): 16252-16257. https://doi.org/10.1002/ange.201808716
[12] Ismail, Marhaina, Mohamad Azmi Bustam, Nor Ernie Fatriyah Kari, and Yin Fong Yeong. "Ideal adsorbed solution theory (IAST) of carbon dioxide and methane adsorption using magnesium gallate metal-organic framework (Mg-gallate)." *Molecules* 28, no. 7 (2023): 3016. https://doi.org/10.3390/molecules28073016
[13] Langmuir, Irving. "The adsorption of gases on plane surfaces of glass, mica and platinum." *Journal of the American Chemical society* 40, no. 9 (1918): 1361-1403. https://doi.org/10.1021/ja02242a004
[14] Ullah, Sami, Mohamad Azmi Bustam, Mohammed Ali Assiri, Abdullah G. Al-Sehemi, Muhammad Sagir, Firas A. Abdul Kareem, Ali EI Elkhalifah, Ahmad Mukhtar, and Girma Gonfa. "Synthesis, and characterization of metal-organic frameworks-177 for static and dynamic adsorption behavior of CO2 and CH4." *Microporous and Mesoporous Materials* 288 (2019): 109569. https://doi.org/10.1016/j.micromeso.2019.109569
[15] Freundlich, Herbert Max Finley. "Over the adsorption in solution." *J. Phys. chem* 57, no. 385471 (1906): 1100-1107.
[16] Sips, Robert. "On the structure of a catalyst surface." *The journal of chemical physics* 16, no. 5 (1948): 490-495. https://doi.org/10.1063/1.1746922
[17] Guarín Romero, Jhonatan R., Juan Carlos Moreno-Piraján, and Liliana Giraldo Gutierrez. "Kinetic and equilibrium study of the adsorption of CO2 in ultramicropores of resorcinol-formaldehyde aerogels obtained in acidic and basic medium." *C* 4, no. 4 (2018): 52. https://doi.org/10.3390/c4040052
[18] Tóth, József. "State equation of the solid-gas interface layers." *Acta chim. hung.* 69 (1971): 311-328.
[19] Mohamed, G., A. Ashraf, and A. Mohamed. "Low-Temperature Adsorption Study of Carbon Dioxide on Porous Magnetite Nanospheres Iron Oxide." *Biointerface Res. Appl. Chem* 12 (2022): 6252-6268. https://doi.org/10.33263/BRIAC125.62526268
[20] Khosrowshahi, Mobin Safarzadeh, Hossein Mashhadimoslem, Hosein Banna Motejadded Emrooz, Ahad Ghaemi, and Mahsa Sadat Hosseini. "Green self-activating synthesis system for porous carbons: Celery biomass wastes as a typical case for CO2 uptake with kinetic, equilibrium and thermodynamic studies." *Diamond and Related Materials* 127 (2022): 109204. https://doi.org/10.1016/j.diamond.2022.109204
[21] Yang, Fan, Xuancan Zhu, Junye Wu, Ruzhu Wang, and Tianshu Ge. "Kinetics and mechanism analysis of CO2 adsorption on LiX@ ZIF-8 with core shell structure." *Powder Technology* 399 (2022): 117090. https://doi.org/10.1016/j.powtec.2021.117090
[22] Salehi, T., and D. Yousefi Kebria. "Synergy of granular activated carbon and anaerobic mixed culture in phenol bioremediation of aqueous solution." *Iranica Journal of Energy & Environment* 11, no. 3 (2020): 178-185. https://doi.org/10.5829/IJEE.2020.11.03.01
[23] Tang, Bin, Xi Lu, Jinfeng Wang, Hao Yu, Yanchao Zhu, Steven E. Atkinson, and Xungai Wang. "Kinetic and thermodynamic studies on gas adsorption behaviour of natural fibres." *The Journal of The Textile Institute* 112, no. 9 (2021): 1390-1402. https://doi.org/10.1080/00405000.2020.1817292
[24] Shahrom, Maisara Shahrom Raja, Cecilia Devi Wilfred, and Fai Kait Chong. "Thermodynamic and kinetic studies on CO2 capture with Poly [VBTMA][Arg]." *Journal of Physics and Chemistry of Solids* 116 (2018): 22-29. https://doi.org/10.1016/j.jpcs.2018.01.008
[25] Raganati, Federica, Michela Alfe, Valentina Gargiulo, Riccardo Chirone, and Paola Ammendola. "Kinetic study and breakthrough analysis of the hybrid physical/chemical CO2 adsorption/desorption behavior of a magnetite-based sorbent." *Chemical Engineering Journal* 372 (2019): 526-535. https://doi.org/10.1016/j.cej.2019.04.165
[26] Wang, Jiawei, Liangying Li, Lidong Guo, Yingcai Zhao, Danyan Xie, Zhiguo Zhang, Qiwei Yang, Yiwen Yang, Zongbi Bao, and Qilong Ren. "Adsorptive Separation of Acetylene from Ethylene in Isostructural Gallate-Based Metal–Organic Frameworks." *Chemistry–A European Journal* 25, no. 68 (2019): 15516-15524. https://doi.org/10.1002/chem.201903952
[27] Basak, Munmun, Md Lutfor Rahman, Md Farid Ahmed, Bristy Biswas, and Nahid Sharmin. "The use of X-ray diffraction peak profile analysis to determine the structural parameters of cobalt ferrite nanoparticles using Debye-Scherrer, Williamson-Hall, Halder-Wagner and Size-strain plot: Different precipitating agent approach." *Journal of Alloys and Compounds* 895 (2022): 162694. https://doi.org/10.1016/j.jallcom.2021.162694
[28] Raja, Pandian Bothi, Kabilashen Readdyi Munusamy, Veeradasan Perumal, and Mohamad Nasir Mohamad Ibrahim. "Characterization of nanomaterial used in nanobioremediation." In *Nano-bioremediation: fundamentals and applications*, pp. 57-83. Elsevier, 2022. https://doi.org/10.1016/B978-0-12-823962-9.00037-4

[29] Wu, Yanhong, Minhua Su, Jiawei Chen, Zuopeng Xu, Jiafeng Tang, Xiangyang Chang, and Diyun Chen. "Superior adsorption of methyl orange by h-MoS2 microspheres: Isotherm, kinetics, and thermodynamic studies." *Dyes and Pigments* 170 (2019): 107591. https://doi.org/10.1016/j.dyepig.2019.107591

[30] Chen, Yingbi, Jiali Tang, Shixing Wang, Libo Zhang, and Wentong Sun. "Bimetallic coordination polymer for highly selective removal of Pb (II): Activation energy, isosteric heat of adsorption and adsorption mechanism." *Chemical Engineering Journal* 425 (2021): 131474. https://doi.org/10.1016/j.cej.2021.131474